THE JOURNAL OF BIOLOGICAL CHEMISTRY
Vol. 266, No. 26, Issue of September 15, pp. 17112-17123, 1991
Printed in U.S.A.

Polyene Fatty Acid Interactions with Recombinant Intestinal and Liver Fatty Acid-binding Proteins

SPECTROSCOPIC STUDIES*

(Received for publication, October 1, 1990)

Gyorgy Nemecz, John R. Jefferson‡, and Friedhelm Schroeder§

From the Division of Pharmacology and Medicinal Chemistry, Department of Pharmacology and Cell Biophysics, University of Cincinnati Medical Center, Cincinnati, Ohio 45267-0004

Binding and proximity relationships of fatty acids with recombinant rat liver fatty acid-binding protein (L-FABP) and intestinal fatty acid-binding protein (I-FABP) were studied with absorption and fluorescence spectroscopy. Protein aromatic amino acids were examined in the absence and presence of bound fatty acid. Second derivative absorbance spectroscopy of the apo- and holoproteins suggested that fatty acid binding altered the conformation of L-FABP, but not of I-FABP. Fatty acid binding also blocked the accessibility of L-FABP tyrosine and I-FABP tryptophan to Stern-Volmer quenching by acrylamide, indicating that these amino acids were present in the fatty acid-binding pocket. Forster energy transfer from I-FABP tryptophan to bound *cis*-parinaric acid resulted in quenching of tryptophan lifetime and appearance of sensitized lifetime of bound *cis*-parinaric acid. The calculated donor-acceptor distances were 16.9 ± 0.6 and 19.2 ± 0.3 Å for I-FABP and L-FABP, respectively. Absorbance spectral shifts and ratios of fluorescence excitation maxima indicated that the parinaric acid microenvironment in the fatty acid-binding site of I-FABP was much less polar than that of L-FABP. Parinaric acids displayed similar rotational correlation time and limiting anisotropy when bound to I-FABP and to L-FABP. These results are consistent with a close proximity of bound fatty acids to the tyrosine and tryptophan residues and with immobilization of the polyene fatty acids in the fatty acid-binding site(s) of L-FABP and I-FABP. The two proteins differ in that only L-FABP has two fatty acid-binding sites and appears to undergo significant conformational change upon fatty acid binding.

The cytosol of various mammalian cells contains a highly abundant 14-15-kDa protein that binds amphiphilic ligands such as fatty acid, fatty acyl-CoA, cholesterol, etc. (recently reviewed in Refs. 1-6). Although the physiological function of the fatty acid-binding proteins (FABPs)[1] is unknown, they are primarily thought of as intracellular fatty acid or hydrophobic ligand carriers, stimulators of lipid (phospholipid, triglyceride, or cholesterol ester) synthetic enzymes, and protectors of free fatty acid-sensitive proteins. Moreover, recent developments indicate that the FABPs may also be part of a family of proteins that regulate gene expression (1) as do other hydrophobic ligand-binding proteins (7, 8). A number of observations are consistent with a potential role of FABPs in gene regulation. Liver (L-FABP) and heart fatty acid-binding proteins have been detected in the cell nucleus (9). L-FABP is identical to protein 14, also called mitosis-associated protein (10, 11). Mammary tumor inhibitory factor has also been identified as a fatty acid-binding protein (12, 13). A most exciting finding is that tyrosine of the adipocyte fatty acid-binding protein is phosphorylated by the insulin receptor upon activation; and thus, this FABP may be involved in regulation of insulin action (14, 15). Clearly, knowledge of both the ligand specificity and the properties of the lipid-binding site(s) of FABPs is necessary for understanding the function of these proteins (16, 17). One of the most challenging problems in identifying ligand specificity and its role in lipid-activated transcriptional regulation is understanding the dynamic protein structural changes following ligand binding (5, 7). The tertiary structure derived from x-ray crystal data of only one of these proteins, the holo and apo forms of intestinal fatty acid-binding protein (I-FABP), has been resolved in detail (18-21). A preliminary report on x-ray crystal structure of L-FABP has also appeared (22). This study was conducted to obtain information on the effect of fatty acid binding on the comparative solution structure of L-FABP and I-FABP. In addition, the fatty acid-binding sites of these proteins are compared using fluorescent *cis*- and *trans*-parinaric acids as spectroscopic reporters of the protein-binding sites. Fluorescence properties of these 18-carbon chain length fatty acids have been described (23-26). These polyene fatty acids also appear to be useful probes of lipid-protein interactions (16, 25, 26).

EXPERIMENTAL PROCEDURES

Materials—[9,10-^{3}H]Oleic acid (10 Ci/mmol) was purchased from Amersham Corp. *trans*-Parinaric acid and *cis*-parinaric acid were obtained from Molecular Probes (Eugene, OR); oleic acid and linoleic acid were from Sigma. Lipidex 1000 was obtained from Pharmacia LKB Biotechnology Inc. Stock solutions of parinaric acids in ethanol were kept at −70 °C under N_2 to prevent oxidation. *N*-Acetyl-L-tryptophanamide and bovine serum albumin (fatty acid-poor, fraction

* This work was supported in part by National Institutes of Health Grant DK41402. The experiments and analyses of tryptophan lifetime were performed at the Laboratory for Fluorescence Dynamics (LFD) at the University of Illinois at Urbana-Champaign (UIUC). The LFD is supported jointly by the Division of Research Resources of the National Institutes of Health under Contract RR03155-01 and the UIUC. The costs of publication of this article were defrayed in part by the payment of page charges. This article must therefore be hereby marked "*advertisement*" in accordance with 18 U.S.C. Section 1734 solely to indicate this fact.

‡ Supported by a postdoctoral fellowship from Lipid Research Training Grant HL07460 and also supported in part by American Heart Association Ohio Affiliate Fellowship SW-91-27-F.

§ To whom correspondence should be addressed.

[1] The abbreviations used are: FABPs, fatty acid-binding proteins; L-FABP, rat liver FABP; I-FABP, rat intestinal FABP; dimethyl-POPOP, 1,4-bis[2-(4-methyl-5-phenyloxazolyl)]benzene.

V) were from Sigma. Dimethyl-POPOP and *p*-terphenyl were obtained from Research Products International Corp. (Elk Grove Village, IL) and stored as stock solution in ethanol and cyclohexane, respectively, at −20 °C and protected from light. All other chemicals were reagent-grade or better.

Protein Purification—Recombinant rat I-FABP and L-FABP were obtained from *Escherichia coli* host strains carrying plasmid pJBL2 (for L-FABP) or plasmid pIFABPexp6 (for I-FABP) (27, 28). These strains were generously provided by Dr. John B. Lowe (Department of Pathology, University of Michigan, Ann Arbor, MI). The protein isolation procedure was identical to that described earlier by Lowe *et al.* (27, 28). Purified recombinant rat I-FABP and L-FABP were delipidated by the procedure of Glatz and Veerkamp (29) modified as described earlier (30). Purity of the proteins was checked with sodium dodecyl sulfate-polyacrylamide electrophoresis (27, 28). Protein was determined by the method of Bradford (31) using the Bio-Rad protein assay kit and corrected as compared to quantitative amino acid analysis (28) or to UV extinction coefficient (32).

L-FABP and I-FABP Tyrosine Microenvironment Polarity: Second Derivative Absorbance Spectroscopy—The degree of polarity (α) of protein tyrosine was calculated according to Equation 1 (33):

$$(\alpha) = (r_n - r_a)/(r_u - r_a) \quad (1)$$

where r_n and r_u are the numerical values of the ratio a/b (a = peak-to-peak distance between the maximum at 287 nm and the minimum at 283 nm, and b = peak-to-peak distance between the maximum at 295 nm and the minimum at 290.5 nm; r_n and r_u are the native and unfolded protein, respectively), and r_a is the a/b value of a mixture containing the same molar ratio of aromatic amino acids dissolved in a solvent similar to the interior of the protein matrix. In this study, r_n was determined from the second derivative spectrum of the protein in the absence and presence of fatty acid ligand, whereas the values of r_a and r_u are those that were reported by Ragone *et al.* (33) for the appropriate ratio of the model compounds *N*-acetyl-L-tryptophanamide and *N*-acetyl-L-tyrosinamide in solvents containing either 6.0 M guanidinium chloride or ethylene glycol to represent fully exposed (high polarity) and fully shielded (low polarity) environments, respectively.

Second derivative spectra were from a DMS 100 UV-visible spectrophotometer (Varian Instruments, Sunnyvale, CA) at 24 °C. Spectroscopic measurement of protein was corrected for light scatter (for I-FABP at 280 nm, ϵ = 1.19 ml mg^{-1} cm^{-1}; for L-FABP at 280 nm, ϵ = 0.45 ml mg^{-1} cm^{-1}) (21). I-FABP and L-FABP were diluted from a stock of delipidated FABP to ~20 μM with buffer (20 mM Tris, 50 mM KCl (pH 7.4)) (32). Spectra for L-FABP were also taken at higher concentration (135 μM) in 25 mM potassium phosphate, 0.02% NaN_3 (pH 7.2) to improve signal/noise. Spectra were scanned at the slowest possible speed, and multiple scans were performed and averaged when needed. Oleic acid was added from a stock solution (10 mM oleic acid in 95% ethanol) either directly or as a film dried in a glass test tube. Ethanol at the concentrations employed did not interfere with the assay.

In the case of L-FABP, second derivative spectral interpretation could not be directly used since this protein lacks tryptophan. Ragone *et al.* (33) showed that the tryptophan contributions to the second derivative spectra are independent of solvent environment and are additive. The spectral contribution of tryptophan was added to L-FABP in a manner similar to that described for other protein systems lacking trytrophan residues (34).

L-FABP and I-FABP Tyrosine Exposure: Stern-Volmer Quenching—Stern-Volmer quenching with acrylamide was as detailed earlier (35, 36) and in Equation 2:

$$F/F_0 = \sum f_i/((1 + K_{di}[Q])(1 + K_{si}[Q])) \quad (2)$$

where K_{di} is the Stern-Volmer dynamic quenching constant of component i, and K_{si} is the static quenching constant. The curves were analyzed by a nonlinear least-squares program including different options for quenching model systems (generously provided by Dr. M. Eftink, University of Mississippi, University, MS). Downward curvature in the quenching curve is interpreted as the fluorophore not being completely accessible to the quencher. Quenching of two populations of fluorophore, one which is accessible to quencher, was analyzed using a modified form of the Stern-Volmer equation (35).

Spectral Measurements—Absorption spectra were measured at 25 °C with either a DMS 100 spectrophotometer or a UVICON 930 spectrophotometer (courtesy of Dr. J. Ball, Department of Pharmacology and Cell Biophysics, University of Cincinnati). The sample absorbance was kept <0.15.

Fluorescence spectra were recorded on an SLM/Aminco SPF 500 spectrophotometer (courtesy of Dr. J. Ball) at 25 °C. Excitation was at 324 nm for *cis*-parinaric acid, 318 nm for *trans*-parinaric acid, 280–285 nm for L-FABP (Tyr), and 285–290 nm for I-FABP (Tyr and Trp). Excitation and emission slit widths were 4 and 10 mm, respectively. Spectra were corrected for excitation monochromator and lamp intensity. Data were collected by an IBM PS/2 computer using an ADC interface and SLM 500 software. The sample protein concentration was varied between 10 and 15 μg/ml (absorbance <0.15) to eliminate inner filter effects and to reduce light scattering. Light scattering was also reduced by use of appropriate cutoff filters. Spectral noise was removed by computer curve smoothing.

Energy Transfer Data Analysis—Energy transfer and Forster distance between donor and acceptor (37) were determined as described earlier (38, 39). The quenching of I-FABP tryptophan and tyrosine fluorescence by *cis*- or *trans*-parinaric acid is a case of energy transfer from different donors to a single acceptor. The donor-acceptor separation (R in angstroms) is:

$$R = R_0((1 - E)/E)^{1/6} \quad (3)$$

where E is energy transfer efficiency, and R_0 is the distance for 50% transfer efficiency. The Forster critical distance (R_0 in angstroms) is:

$$R_0 = (JQ_0\kappa^2n^{-4})^{1/6}(9.79 \times 10^3) \quad (4)$$

where J = spectral overlap of donor emission and acceptor absorption spectra; κ^2 (orientation factor) = ⅔, the dynamic average (40); n = the refractive index (for aromatic amino acids in the interior of proteins, n = 1.416) (25); and Q_0 = quantum yield of donor in absence of acceptor. For κ^2 to equal ⅔, it is necessary that: 1) the average angle between donor-acceptor pair dipole moment should be near 30°, and 2) the polarization of the donor-acceptor pair should be <0.3 (41–43). Quantum yields of I-FABP tryptophan and L-FABP tyrosine, determined relative to dimethyl-POPOP (1 μM in cyclohexane, quantum yield of 0.93) (44), were 0.294 and 0.0658, respectively. The spectral overlap (J) was calculated according to the method of Stryer (41) as described earlier (38, 39):

$$J = \int F_d(\lambda)\epsilon_a(\lambda)\lambda^4\, d\lambda \Big/ \int \lambda F_d(\lambda)\, d\lambda \quad (5)$$

where ϵ_a = extinction coefficient of the acceptor, λ = wavelength range of spectral overlap, and F_d = the fluorescence intensity of the donor.

The efficiency of energy transfer (E) is related to the intensity of donor fluorescence in the absence (F_d^0) and presence (F_d) of the acceptor:

$$E = 1 - (F_d/F_d^0) \quad (6)$$

Fluorescence Lifetime Determination of Parinaric Acids—Fluorescence lifetimes of *cis*- and *trans*-parinaric acids were determined with an SLM 4800 subnanosecond spectrofluorometer modified to 1–250-MHz multifrequency capability (ISS Inc., Urbana, IL) as described earlier (45). The excitation source was a helium/cadmium laser (Model 4240NB, Liconix, Sunnyvale, CA) with emission at 325 nm. During fluorescence lifetime analysis, the excitation polarizer was set at 0 °C and the emission polarizer was set at 55 °C (to eliminate brownian motion as a determinant of apparent lifetime). The inner filter effect was avoided by diluting all samples such that the absorbance at 325 nm (the excitation wavelength) was <0.15. Scattered light was reduced by setting the emission polarizer at 55 °C, by use of dilute solutions, and by use of a sharp cutoff filter (Janos GG-375) in the emission system. Temperature was maintained at 25 °C.

Fluorescence Lifetime Determination of Tryptophan in I-FABP—Tryptophan lifetime measurements were made at the Laboratory for Fluorescence Dynamics (Department of Physics, University of Illinois, Champaign-Urbana, IL). Lifetime determinations were performed with a multifrequency cross-correlation phase and modulation fluorometer, which uses the harmonic content of a high repetition rate mode-locked Antares Model 76-MSHG neodymium/YAG laser (Coherent Inc., Palo Alto, CA). To obtain tryptophan excitation at 295 nm, this laser was used to excite a dye (rhodamine 6G) in a Model 700 dye laser (Coherent Inc.) synchronously pumped and cavity-dumped. The pulse train of the laser was frequency-doubled with an angle-tuned Model 390 frequency doubler (Spectra-Physics Inc., Mountain View, CA) using a KDP crystal. The excitation was chosen at 295 nm to eliminate the contribution of tyrosyl residues to the total fluorescence. Emission was observed through one of two types of filters: for tryptophan emission, a U360 band-pass filter (Hoya Optics Inc., Fremont, CA); and for sensitized parinaric acid emission (due to energy transfer from I-FABP tryptophan to bound parinaric acid), a KV389 cutoff filter. These filters also cut off Raman emission at 311 nm.

Fluorescence Lifetime Data Acquisition and Analysis—Fluorescence lifetime data were acquired and analyzed as described earlier (45). Data were obtained at 8–12 modulation frequencies (20–140 MHz) using an external lifetime standard of dimethyl-POPOP (1.45 ns) or *p*-terphenyl (1.0 ns). Data were acquired until the limit of standard error was reached for phase and modulation at 0.2° and 0.04, respectively. Data were collected and analyzed with ISS-187 and Global software (ISS Inc.).

The data were fitted to a sum of exponential terms each characterized by a lifetime and fractional intensity (f). The reduced χ^2 parameter was used to judge the "goodness" of fit to the applied model. Data for distributional analysis were best fitted to Lorentzian distribution. Each component distribution was characterized by a lorentzian shape according to the following function:

$$f(\tau) = A/(1 + ((\tau - C)/(W/2))^2) \tag{7}$$

where C is the center of lifetime distribution, W is the width of the lifetime distribution at half-height, τ is the lifetime, A is a constant obtained from the normalization condition, and $f(\tau)$ represents the function that minimizes the reduced χ^2.

Differential Polarized Phase and Modulation Fluorometry—Differential phase and modulation ratio experiments were performed to calculate not only steady-state polarization, but, more important, to resolve steady-state polarization into limiting anisotropy (a measure of restriction to motion or order) and rotational correlation time in nanoseconds (a dynamic parameter reflecting rates of motion). The procedures used were described in detail previously by this laboratory (38, 39, 45, 46) and will not be reiterated here.

RESULTS

Spectral Properties—Both amino acid and spectral analyses indicate that apo I-FABP contains fluorescent aromatic amino acid residues: 4 tyrosines and 2 tryptophans (5, 17). Absorbance of recombinant apo I-FABP was maximal at 281 nm (Fig. 1*A*), whereas fluorescence emission was maximal near 338 nm (Fig. 2*A*, *solid line*). The long-wavelength position of the apo I-FABP tryptophan emission (Stokes shift of 57 nm), the broad emission bandwidth (59 nm), and the high quantum yield (0.294) are all consistent with at least one of the apo I-FABP tryptophans being localized at the I-FABP surface in contact with water (47). This observation was further substantiated by fluorescence lifetime analysis indicating the presence of two lifetime components for I-FABP tryptophan (see below).

Amino acid and spectral analyses indicate that apo L-FABP contains fluorescent aromatic amino acid residues: 3 tyrosines and no tryptophans (5, 17). Absorbance of recombinant apo L-FABP was maximal at 279 nm (Fig. 1*B*), whereas fluorescence emission was maximal near 305 nm (Fig. 2*B*, *solid line*). The smaller Stokes shift (26 nm), narrower emission bandwidth (40 nm), and the lower quantum yield (0.0658) are all consistent with L-FABP structure differing significantly from that of I-FABP.

The degree of exposure of the tyrosine residues in I-FABP along with the effect of fatty acid binding on this parameter were determined by second derivative absorbance spectroscopy as described under "Experimental Procedures." The second derivative spectrum of apo I-FABP in buffer (Fig. 3*A*, *curve 1*) yielded an α value of 0.28. This α value represents the fraction of tyrosine residues exposed to the aqueous solvent (only 1 of the 4), and this value was not affected by adding the fatty acid ligand oleic acid to the system (*curves 2* and *3*). Binding of the nonfluorescent linoleic acid to I-FABP

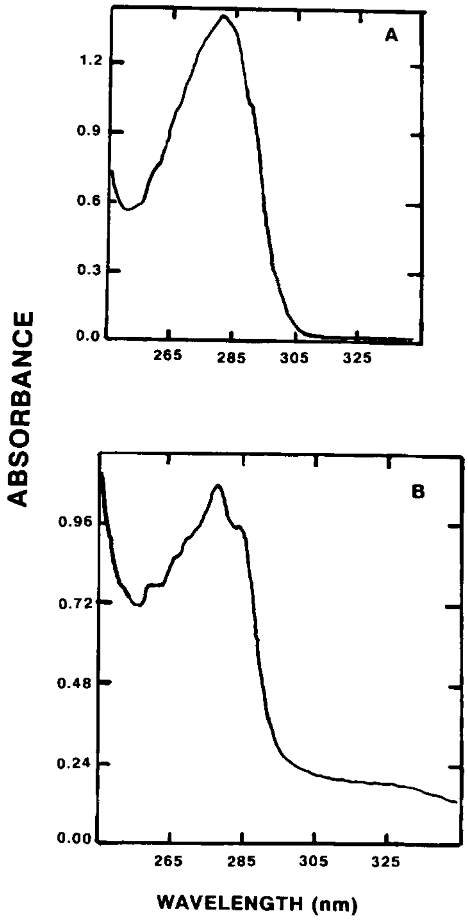

FIG. 1. **Ultraviolet absorption spectra of apo I-FABP and apo L-FABP.** I-FABP (*A*) and L-FABP (*B*) were 77.8 and 135 μM, respectively. Spectra were obtained with 0.5-ml cuvettes and a Varian DMS 100 spectrophotometer.

did not alter tryptophan fluorescence emission (see below, Fig. 7*C*). Thus, I-FABP does not undergo gross conformational change upon fatty acid binding.

Comparison of the second derivative spectra of holo L-FABP (containing bound oleic acid) (Fig. 3*B*, *curves 2* and *3*) and apo L-FABP (Fig. 3*B*, *curve 1*) indicated a substantial change in tyrosine residue microenvironment. The second derivative spectrum of L-FABP was maximally altered when 2 mol of oleate were added per mol of protein. This value is in close agreement with that obtained by other methods described earlier (30).

Tryptophanyl Emission Decay—The tryptophanyl emission decay in apo and holo I-FABPs was fit to one, two, and three components. For one-component fit, the χ^2 values ranged in excess of 100. The fits were markedly improved by fitting the data for apo I-FABP to two lifetime components near 4.6 (0.8 fractional intensity) and 1.7 ns (0.2 fractional intensity) (Table I). Inclusion of a light-scattering component (τ_3 fixed at 0.001 ns) further improved χ^2 and increased the two lifetimes for tryptophan slightly to 5.2 and 2.5 ns, respectively, while dramatically altering the fractional intensities to 0.58 and 0.41, respectively (Table I). Thus, the data best fit two lifetime components with nearly equal fractional intensities (Table I) and pre-exponential terms (data not shown). Binding of oleic acid did not alter either the two lifetimes or the fractional intensities. In contrast, in the presence of bound *cis*-parinaric acid or bound *trans*-parinaric acid, the long and short lifetime components were both decreased, with the larger effect (41.3 *versus* 13% decrease) observed on the

TABLE I
Discrete component analysis of I-FABP tryptophan emission decay
I-FABP = 4.8 μM; fatty acid = 20 μM. τ, fluorescence lifetime in nonoseconds; f, fractional intensity. Excitation was at 295 nm. Emission was monitored through a U360 band-pass filter to eliminate *cis*- or *trans*-parinaric acid-sensitized emission.

Fatty acid	τ_1	f_1	τ_2	f_2	τ_3	f_3	χ^2
Two-component fit							
None	4.59	0.80	1.68	0.20			3.57
Oleic	4.66	0.80	1.50	0.20			4.11
cis-Parinaric	4.17	0.89	0.54	0.11			6.27
trans-Parinaric	4.08	0.87	0.42	0.13			12.9
Three-component fit							
None	5.23	0.58	2.47	0.41	0.001	0.01	1.08
Oleic	5.22	0.63	2.22	0.36	0.001	0.01	0.89
cis-Parinaric	4.50	0.80	1.45	0.16	0.001	0.04	1.33
trans-Parinaric	4.57	0.74	1.57	0.20	0.001	0.06	2.86

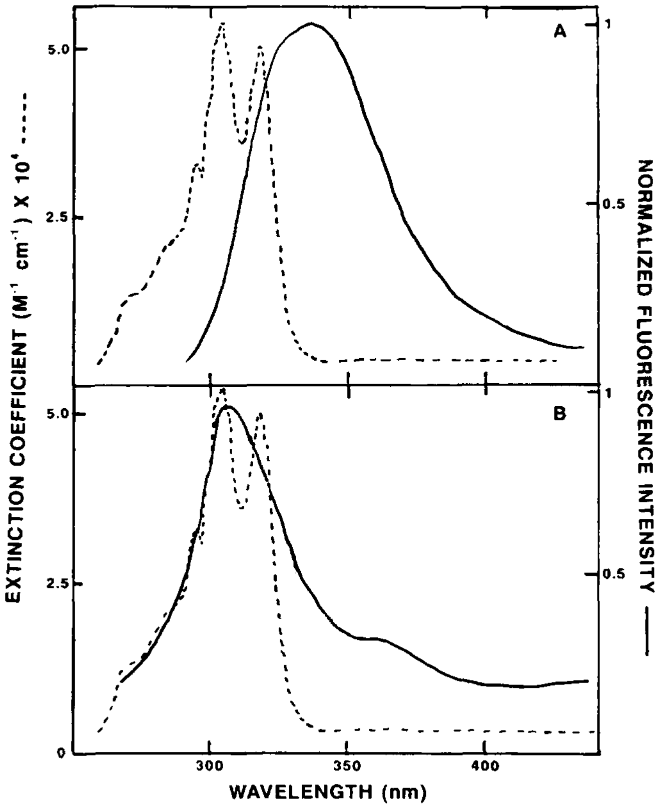

FIG. 2. **I-FABP and L-FABP fluorescence emission spectra: overlap with *cis*-parinaric acid absorption.** Fluorescence emission spectra of 2 μM I-FABP (*A*, ——) and 9 μM L-FABP (*B*, ——) were obtained with excitation at 295 and 282 nm, respectively, as described under "Experimental Procedures." Absorption spectra of 1 μM *cis*-parinaric acid (- - -) bound to I-FABP or L-FABP (also determined as described under "Experimental Procedures") are superimposed on each panel to demonstrate overlap.

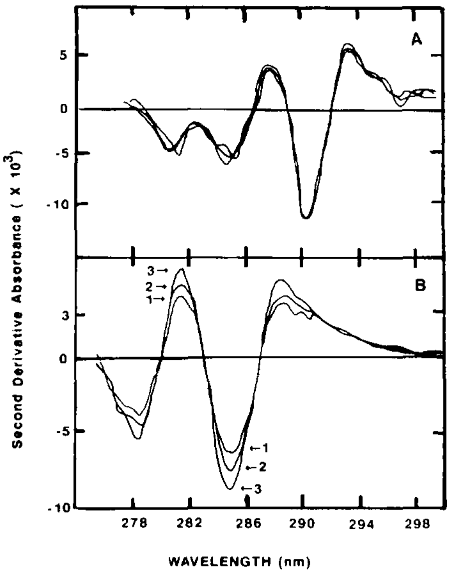

FIG. 3. **Second derivative absorption spectra of apo and holo I-FABPs and L-FABPs.** *A*, second derivative absorption spectra of delipidized apo I-FABP (*curve 1*) and holo I-FABP with bound oleic acid were obtained as described under "Experimental Procedures." I-FABP was 23 μM, and oleic acid concentrations were 0 μM (*curve 1*), 46 μM (*curve 2*), and 60 μM (*curve 3*). Curves were not labeled due to overlap. *B*, second derivative absorption spectra of delipidized apo L-FABP (*curve 1*) and holo L-FABP with bound oleic acid were obtained as described under "Experimental Procedures." L-FABP was 25.2 μM and oleic acid concentrations were 0 μM (*curve 1*), 28 μM (*curve 2*), and 73 μM (*curve 3*).

shorter lifetime component. It should be noted that, in the presence of the parinaric acids (but not oleic acid), the fractional intensities of the two components were dramatically shifted in favor of the longer lifetime component.

The Lorentzian analysis for one ($\chi^2 = 2.1$) (Fig. 4*A*)-, two ($\chi^2 = 1.3$) (Fig. 4*B*)-, or three ($\chi^2 = 1.4$) (Table II)-component fit provided lower χ^2 values than did the respective discrete component analysis (see Table I). The three-component fit did not, however, significantly improve χ^2 as compared to the two-component fit (Table II). In either case, the two lifetimes obtained for tryptophan in apo I-FABP (4.3 and 1.9 ns) were basically similar to those obtained by the discrete component analysis. *cis*-Parinaric acid and *trans*-parinaric acid (but not oleate) reduced both lifetime components and preferentially reduced the fractional contribution of the shorter lifetime component. In the presence of parinaric acids, the distributional width of the long and primarily the short lifetime components was increased (two-component analysis) (Table II). This observation is shown graphically in Fig. 4, where the distribution width is increased by *cis*-parinaric acid (Fig. 4, *C versus A*; and *D versus B*).

As shown above, tryptophan lifetime in I-FABP can best be described by two components. It has been shown that in another two-tryptophan protein, liver alcohol dehydrogenase, the longer lifetime component is assigned to the more aqueous exposed residue (48). Ligand binding alone (oleic acid) did not alter the conformation of the protein, as indicated by unaltered fluorescence lifetime properties of tryptophan. However, in the presence of parinaric acids, the lifetimes, fractional intensities, and distributional widths of I-FABP tryptophan were altered. That these effects were due to energy transfer from I-FABP tryptophan to the conjugated tetraene near the methyl end of the parinaric acids is confirmed by the observation of sensitized emission lifetime of *cis*-parinaric acid and bound *trans*-parinaric acid when bound to I-FABP (Table III). Aqueous unbound parinaric acids did not fluoresce. The sensitized emission decay of bound *cis*-parinaric acid better fit three (as compared to one or two) lifetime components near 8.8, 2.9, and 0.48 ns in the discrete analysis. These lifetimes were similar to those obtained when the bound *cis*-parinaric acid was excited directly at 324 nm (see Table VII below). Lorentzian analysis did not, however, improve the fit.

In summary, the difference in the magnitude of the quenching of fluorescence lifetime effects of the two components probably reflects the contribution of the 2 specific indole residues. A similar observation has been made for bound heme quenching of the 2 tryptophan residues in sperm whale myoglobin (49). X-ray crystallographic evidence also indicates that the 2 tryptophanyl residues of I-FABP, although very close in structure, are located in different microenvironments (19). One of these, Trp-86, appears to be within the fatty acid-binding site, whereas the other, Trp-6, appears further removed and more exposed to the aqueous (19).

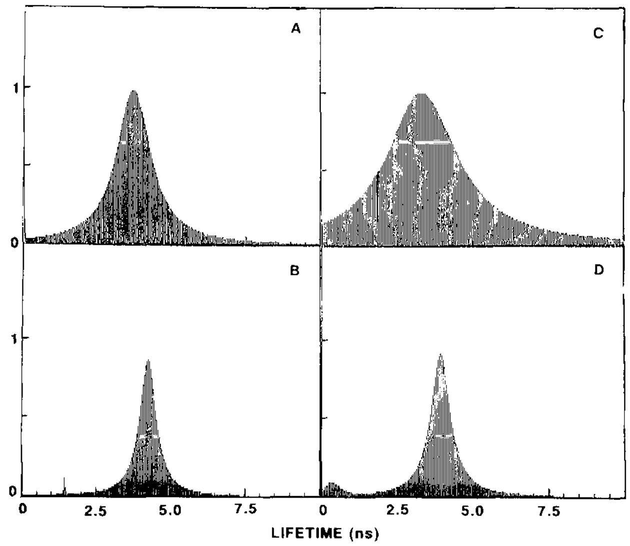

FIG. 4. **Tryptophanyl fluorescence lifetime distribution of apo and holo I-FABPs.** I-FABP was 4.8 μM; *cis*-parinaric acid was 20 μM. *A*, apo I-FABP one-component; *B*, apo I-FABP two-component; *C*, holo I-FABP one-component; *D*, holo I-FABP two-component.

Acrylamide Quenching—The exposure of I-FABP aromatic amino acid residues to acrylamide, an aqueous quencher, was determined. Essentially, all of the tryptophan was available for the quencher in apo I-FABP (Fig. 5*A*, *open circles*). At low concentration of fatty acid, the quenching effect of acrylamide was weakened, but did not change the shape of the Stern-Volmer curve. At high concentration of fatty acid when the binding site was fully saturated, the Stern-Volmer plot showed downward curvature expressing the difference in the accessibility between the 2 tryptophans. The single Stern-Volmer quenching constants obtained from Equation 2 (see "Experimental Procedures") were 3.9 for apo I-FABP, 2.9 for holo I-FABP (2.25 μM oleic acid), and 2.2 ($\chi^2 = 5.2 \times 10^{-4}$) for holo I-FABP (18 μM oleic acid) (Table II). When the latter curve (fully saturated binding site) was analyzed for two components, a better fit was obtained ($\chi^2 = 9.6 \times 10^{-5}$), and the quenching parameters were $k_1 = 0.33$, $k_2 = 3.07$, $f_1 = 0.23$, and $f_2 = 0.77$. As indicated by decreased slope and shape of the curve, oleate binding decreased the accessibility of 1 of the 2 tryptophan residues of I-FABP to acrylamide. Thus, at least 1 of the tryptophans must be located deep within the fatty acid-binding pocket when saturating concentrations of fatty acid are available to the fatty acid-binding site. X-ray crystal data indicate that Trp-82 is located in the fatty acid-binding site (19), which apparently accommodates the fatty acid so closely that it does not allow acrylamide penetration to the tryptophan in the fatty acid-binding site.

The Stern-Volmer quenching constant obtained with equations modified for downward curvature of Stern-Volmer plots was 3.6 for apo I-FABP (Fig. 5*B*, *open circles*), 3.0 for holo L-FABP (*filled circles*, 9 μM oleic acid), and 2.58 for holo L-FABP (*open triangles*, 18 μM oleic acid) (Table IV). The acrylamide-accessible fraction of tyrosine in holo L-FABP containing 18 μM oleic acid was 0.71. In the case of apo L-FABP, the accessible fraction of tyrosine fluorescence was ~0.9. Since there are 3 tyrosine residues in L-FABP, these data are consistent with at least 1 tyrosine being aqueous solvent-inaccessible. As indicated by decreased slopes of the Stern-Volmer plots in holo *versus* apo L-FABP, saturation of the two fatty acid-binding sites of L-FABP with oleic acid decreased the accessibility of tyrosine to acrylamide. At least 1 L-FABP tyrosine is shielded from acrylamide quenching by the bound oleic acid.

Spectral Properties of Bound Parinaric Acids—Absorption spectra of *cis*-parinaric acid bound to I-FABP displayed maxima near 326 and 311 nm with a shoulder at 296 nm (Fig. 6*A*). Titrating the fatty acid-binding sites on I-FABP with increasing concentrations of *cis*-parinaric acid (between 0.5 and 5 μM) resulted in significant absorption maxima shifts

TABLE II

Continuous lorentzian distributional analysis of I-FABP tryptophan emission decay

I-FABP = 4.8 μM; fatty acid = 20 μM. *C*, center of lifetime distribution in nanoseconds; *W*, width of lifetime distribution in nanoseconds; *f*, fractional intensity. Excitation was at 295 nm. Emission was monitored through a U360 band-pass filter to eliminate *cis*- or *trans*-parinaric acid-sensitized emission.

Fatty acid	C_1	W_1	f_1	C_2	W_2	f_2	C_3	W_3	f_3	χ^2
Two-component fit										
None	4.27	0.63	0.86	1.88	0.21	0.14				1.34
Oleic	4.13	0.97	0.91	1.42	0.05	0.09				1.10
cis-Parinaric	3.82	1.03	0.92	0.16	1.70	0.08				1.60
trans-Parinaric	3.90	0.91	0.89	0.14	0.67	0.09				3.38
Three-component fit										
None	4.82	0.37	0.71	1.94	0.05	0.27	0.001	0.05	0.01	1.40
Oleic	5.11	0.22	0.65	2.24	0.05	0.34	0.001	0.09	0.01	0.85
cis-Parinaric	4.52	0.06	0.79	1.61	0.12	0.17	0.001	0.14	0.04	1.08
trans-Parinaric	4.62	0.05	0.72	1.73	0.19	0.21	0.001	0.05	0.09	2.97

TABLE III

Sensitized emission of cis-parinaric acid bound to I-FABP

I-FABP = 4.8 μM; *cis*-parinaric acid = 20 μM. In the discrete analysis, τ = lifetime in nanoseconds, whereas f = fractional intensity. In the lorentzian distributional analysis, C = center of lifetime distribution, W = width of lifetime distribution, and f = fractional intensity. Excitation was at 295 nm. All emission measurements were made with a KV389 cutoff filter (Schott Glass Technologies Inc., Duryea, PA) to eliminate tryptophan emission.

Discrete component analysis										
Two-component fit				Three-component fit						
τ_1	f_1	τ_2	χ^2	τ_1	f_1	τ_2	f_2	τ_3	f_3	χ^2
4.45	0.43	0.52	10.6	8.8	0.14	2.9	0.34	0.48	0.52	3.8

Lorentizian distributional analysis															
Two-component fit						Three-component fit									
C_1	W_1	f_1	C_2	W_2	χ^2	C_1	W_1	f_1	C_2	W_2	f_2	C_3	W_3	f_3	χ^2
4.8	0.05	0.20	0.41	1.48	10.4	5.2	0.06	0.30	1.6	0.06	0.01	0.59	0.65	0.69	3.8

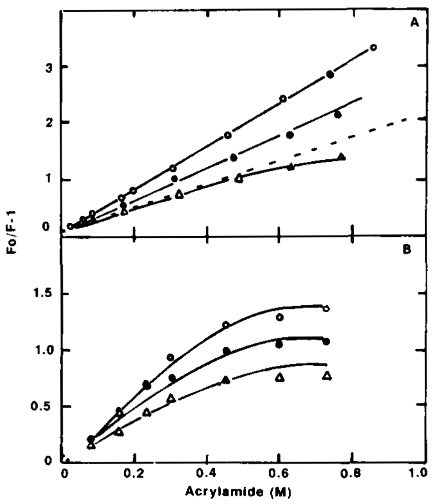

FIG. 5. **Acrylamide quenching of tryptophan and tyrosine fluorescence in apo and holo I-FABPs and L-FABPs.** *A*, acrylamide quenching of tryptophan fluorescence in delipidized apo I-FABP and holo I-FABP containing oleic acid was performed as described under "Experimental Procedures." I-FABP was 4.3 μM, and oleic acid concentrations were 0 μM (○), 2.25 μM (●), and 9 μM (△). The results are presented as Stern-Volmer plots. F_0 and F represent the fluorescence of I-FABP (excitation at 295 nm and emission at 338 nm) in the absence and presence of quencher, respectively. *B*, acrylamide quenching of tyrosine fluorescence in delipidized apo L-FABP and holo L-FABP containing oleic acid was performed as described under "Experimental Procedures." L-FABP was 4.5 μM, and oleic acid concentrations were 0 μM (○), 9 μM (●), and 18 μM (△). The results are presented as Stern-Volmer plots. F_0 and F represent the fluorescence of L-FABP (excitation at 285 nm and emission at 308 nm) in the absence and presence of quencher, respectively.

TABLE IV

Acrylamide quenching of I-FABP and L-FABP aromatic acids: Stern-Volmer quenching constants

K_{sv} is the Stern-Volmer quenching constant; K is the apparent quenching constant of the accessible fraction. Curves were fit to single components determined from the plot of $F_0/\Delta F$ *versus* $1/[Q]$.

Oleic acid	I-FABP K_{sv}	L-FABP K
μM	M^{-1}	M^{-1}
0	3.9	3.6
2.25	2.9	
9.0		3.0
18	2.2 ($\chi^2 = 5.4 \times 10^{-4}$)	2.6
18[a]	0.33, 3.07 ($\chi^2 = 1.6 \times 10^{-5}$)	

[a] Two-component fit as described under "Experimental Procedures."

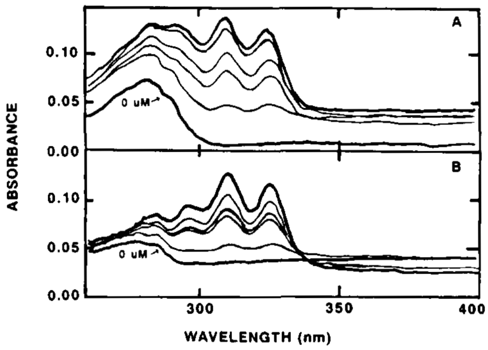

FIG. 6. **Effect of interaction with I-FABP and L-FABP on absorption spectra of *cis*-parinaric acid.** Shown are the absorption spectra of FABPs in the presence of *cis*-parinaric acid (0.5–4 μM). In *A*, I-FABP was 2 μM, and samples (from *bottom* to *top*) contained 0–3.8 μM *cis*-parinaric acid. In *B*, L-FABP was 1.8 μM, and samples (from *bottom* to *top*) contained 0–3.8 μM *cis*-parinaric acid.

(Fig. 6*A*). The absorption maximum at 326.0 nm was blue-shifted 1.8 nm, and the maximum at 311.4 nm was blue-shifted 1.2 nm. These shifts were due to the appearance of increasing amounts of free parinaric acid in the aqueous buffer upon titration of the I-FABP-binding site. Similar spectral shifts have been observed with parinaric acid binding to albumin (24). The I-FABP A_{326}/A_{310} ratio reached a constant value near 1 eq of added *cis*-parinaric acid. The ratios of fluorescence excitation maxima of *cis*- and *trans*-parinaric acids are highly dependent on solvent dielectric constant (Table V). The ratio of *cis*-parinaric acid fluorescence at 322/294 nm (measured at constant emission wavelength of 420 nm) decreased from 1.56 to 1.26, with solvent dielectric constant increasing from 2 to 42. Similar results were obtained with *trans*-parinaric acid. When either *cis*- or *trans*-parinaric acid was bound to I-FABP, the excitation peak ratios were near 1.4. This ratio corresponded to a fatty acid-binding site microenvironment with a dielectric constant of 16, considerably less polar than that of water (dielectric constant of 80), but more polar than that of a hydrophobic lipid environment such as membrane lipids (dielectric constant of <2).

In contrast, the absorption maxima of *cis*-parinaric acid bound to L-FABP remained constant at 325.5 and 309.5 nm upon titration with *cis*-parinaric acid (Fig. 6*B*). The ratio of the extinction coefficient of the minimum at ~318 nm and the absorption peak at ~310 nm plateaued when the molar ratio of *cis*-parinaric acid to L-FABP was ~2. The L-FABP excitation spectral peak ratio was 1.29, consistent with a fatty

TABLE V

Effect of solvent dielectric constant on spectral peak ratios of cis- and trans-parinaric acids

Fluorescence excitation spectra were obtained as described under "Experimental Procedures." Emission wavelength was 420 nm. The ratio of fluorescence at excitation maxima of 322/294 nm was determined in the solvents below or when fatty acids (0.05 μM) were bound to I-FABP or L-FABP (0.1 μM).

Solvent or environment	Dielectric constant[a]	F_{322}/F_{294}	
		cis-Parinaric acid	*trans*-Parinaric acid
Dioxane	2	1.56	1.56
Dioxane/H_2O			
90:10	5	1.52	1.54
80:20	10	1.45	1.41
70:30	16	1.40	1.38
60:40	25	1.35	1.34
50:50	32	1.28	1.23
40:60	42	1.26	1.24
I-FABP		1.40	1.39
L-FABP		1.29	1.27

[a] Ref. 22.

acid-binding site microenvironment with a dielectric constant of 30. Thus, the microenvironment polarity of parinaric acid fluorophore in the fatty acid-binding site of L-FABP may be much more polar than that of I-FABP.

Forster Energy Transfer from I-FABP to Bound Parinaric Acid—The absorbance spectrum of *cis*-parinaric acid in buffer displayed maxima near 326, 311, and 294 nm (Fig. 2). Emission was maximal near 420 nm (data not shown). The emission spectra of I-FABP upon excitation at 280 and 295 nm generated emission peaks at ~335 and 338 nm, respectively (Fig. 2*A*). The modest degree of overlap between the absorbance spectrum of *cis*-parinaric acid and the emission spectra of I-FABP tryptophan (Fig. 2*A*) allows Forster energy transfer to occur from I-FABP aromatic residues to *cis*-parinaric acid. Upon addition of increasing amount of *cis*-parinaric acid (Fig. 7*A*) or *trans*-parinaric acid (Fig. 7*B*) to I-FABP, the intensity of the protein tryptophan emission maximum was decreased (Fig. 7*A*). I-FABP tryptophan fluorescence quenching was higher with *cis*-parinaric acid than with *trans*-parinaric acid. Although this quenching may be due to change in I-FABP conformation, such conformational changes were not noted with fatty acid binding to I-FABP (see above). In addition, linoleic acid, a nonfluorescent 18-carbon polyunsaturated fatty acid, did not reduce the I-FABP tryptophan emission (Fig. 7*C*), and oleic acid did not reduce I-FABP tryptophan lifetime (see Tables I and II). The efficiency of energy transfer from I-FABP tryptophan to *cis*- and *trans*-parinaric acids was 58 and 32–34%, respectively. The Forster energy transfer distance between I-FABP tryptophan donor and *cis*-parinaric acid acceptor was calculated as described under "Experimental Procedures." The spectral overlap integral (J) for I-FABP-bound *cis*- and *trans*-parinaric acid transfer was 1.08 and 0.94 $\times 10^{-15}$ ml M^{-1}, respectively (Table VI); I-FABP quantum yield was 0.294; and refractive index was assumed as $n = 1.41$ (25). The orientation factor (κ^2) was assumed equal to ⅔ because the fluorescence polarization of the acceptor was <0.3 and the angle of the dipole moment vector between donor and acceptor was calculated to be 30°. The latter calculation was performed as described earlier (41). In any case, assumption of an orientation factor is valid for most proteins, and the probability of the introduced error by the orientation factor is <10%. The Forster distance (R_0 in angstroms) at which 50% transfer occurs was between 17.7 ± 0.3 for *cis*-parinaric acid and 17.6 ± 0.4 for *trans*-parinaric acid (Table VI).

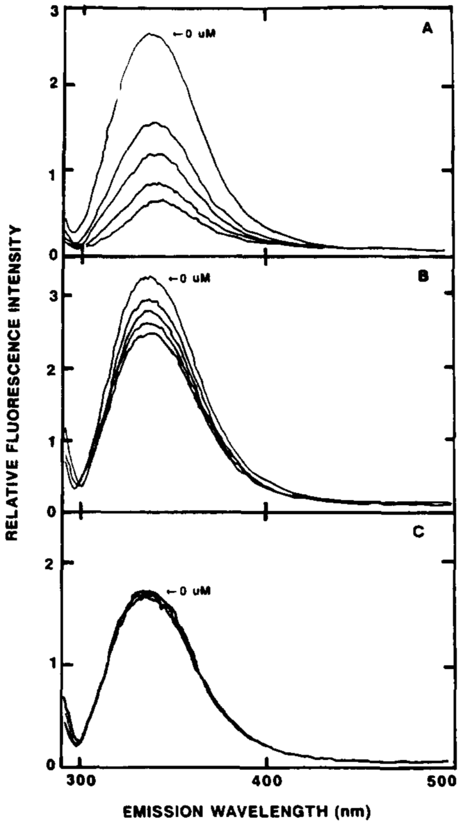

FIG. 7. **Effect of fatty acid binding on fluorescence emission spectra of I-FABP.** Fluorescence emission spectra of I-FABP in the presence of *cis*-parinaric acid (*A*), *trans*-parinaric acid (*B*), and linoleic acid (*C*) were obtained as described under "Experimental Procedures." The I-FABP concentration was 2.8–3.9 μM; the measurements used excitation at 295 nm. The concentrations of fatty acids (from *top* to *bottom*) were as follows: *A*, 0, 4, 8, 12.2, and 16.3 μM; *B*, 0, 3.2, 3.8, 5.6, and 9 μM; *C*, 0, 1, 2, 3.2, and 3.8 μM.

TABLE VI

Forster energy transfer from I-FABP tryptophan and L-FABP tyrosine to bound parinaric acids

J is the overlap integral; R_0 is the Forster distance with 50% probability of energy transfer; E is the transfer efficiency; and R is the calculated distance between donor and acceptor. Values refer to the mean ± S.E., or individual values differed <5% from the mean ($n = 3$).

Donor-acceptor	J	R_0	E	R
	ml M^{-1}	Å	%	Å
I-FABP				
Trp-*cis*-parinaric acid	1.08×10^{-15}	17.7 ± 0.3	58	16.9 ± 0.6
Trp-*trans*-parinaric acid	0.94×10^{-15}	17.6 ± 0.4	33	18.6 ± 0.7
L-FABP				
Tyr-*cis*-parinaric acid	1.20×10^{-14}[a]	20.9 ± 0.2[a]	63	19.2 ± 0.3[a]
Tyr-*trans*-parinaric acid	1.30×10^{-14}[a]	21.2 ± 0.3[a]	75[a]	17.7 ± 0.3

[a] $p < 0.05$ by Student's t test as compared to I-FABP.

Excitation of L-FABP at 282 nm generated an emission peak centered between 305 and 307 nm. The very large overlap between the absorbance spectrum of *cis*-parinaric acid and the emission spectra of L-FABP tyrosine (Fig. 2*B*) is indicated by an overlap integral nearly 10-fold larger than that for I-FABP above (Table VI). This overlap allows Forster energy transfer to occur from L-FABP aromatic residues to *cis*-parinaric acid. Using this overlap integral, a quantum yield of 0.0658 for L-FABP tyrosine, and energy transfer efficiency of 63 and 75% for *cis*- and *trans*-parinaric acids, respectively, the Forster parameters were calculated: R_0 = 19.2 ± 0.3 and 17.7 ± 0.3 Å (Table VI). Energy transfer from L-FABP tyrosine to *cis*- or *trans*-parinaric acid was observed not only as a decrease in the protein fluorescence, but also as a concomitant increase in *cis* (Fig. 9*A*)- or *trans* (Fig. 9*B*)-parinaric acid fluorescence emission at 420 nm upon adding increasing amounts of parinaric acid. Although oleic acid (Fig. 9*C*) did not influence the fluorescence intensity of L-FABP emission at 305 nm as much as parinaric acid, fluorescence did not change significantly or decreased slightly (Fig. 9*C*) when spectra were corrected for background (fatty acid in buffer). The fluorescence emission changes were not fully dependent on concentration of oleic acid. Thus, the above calculated Forster energy transfer distances are complicated, in part, by the conformational changes in L-FABP upon ligand binding.

Three important observations can be made from the energy transfer results summarized in Table VI. 1) The R_0 distances were significantly shorter for the I-FABP tryptophan-parinaric acid donor-acceptor pairs than for the L-FABP tyrosine-parinaric acid donor-acceptor pairs. 2) The distance (R) between I-FABP tryptophan and *cis*-parinaric acid was shorter than that between L-FABP tyrosine and *cis*-parinaric acid. 3) Due to the smaller energy transfer efficiency, the distance (R) between I-FABP tryptophan and *trans*-parinaric acid was not significantly different from that between L-FABP tyrosine and *trans*-parinaric acid. Thus, the *cis*-parinaric unsaturated acid appears to fit more deeply/closely than *trans*-parinaric acid into the I-FABP fatty acid-binding pocket as compared to L-FABP. This difference may account for the lower K_d of *cis*-parinaric acid when bound to I-FABP as compared to L-FABP (0.23 *versus* 0.72 μM; $p < 0.01$) (see Ref. 30).

Parinaric Acid Quenching of I-FABP Tryptophan—The exposure of I-FABP tryptophan to *cis*-parinaric acid quenching was examined. I-FABP has 2 tryptophan residues, both of which are aqueous-exposed as indicated by acrylamide quenching. Although x-ray crystal data indicate that 1 tryptophan is in the fatty acid-binding site of I-FABP (18, 19), it is not known if either or both tryptophan residues are located within the fatty acid-binding site of I-FABP in aqueous solution. A Stern-Volmer plot of *cis*-parinaric acid quenching of I-FABP tryptophan was biphasic (Fig. 8). The Stern-Volmer plot of I-FABP tryptophan fluorescence with increasing *cis*-parinaric acid quencher was not linear and demonstrated an upward curvature. This may indicate the presence of more than one type of quenching. Modified Stern-Volmer plots (see "Experimental Procedures") were constructed to resolve two quenching components, and two quenching constants were determined therefrom (5.067 and 0.0589 M^{-1}, respectively). Extrapolation of the two parts of the Stern-Volmer plot indicate a break point near 5 μM *cis*-parinaric acid (I-FABP was 4.3 μM). Thus, at low *cis*-parinaric acid levels, 1 I-FABP tryptophan may be quenched by a dynamic mechanism, whereas at higher *cis*-parinaric acid levels, a second tryptophan is quenched by a static quenching mechanism. The static quenching constant (quite small) was probably not due to complex formation. Rather, the static component was due to the probability that the second tryptophan in the ground state is adjacent to the quencher. Since the single I-FABP fatty acid-binding site is occupied above 5 μM *cis*-parinaric acid, the second I-FABP tryptophan may be outside the fatty acid-binding site.

Fluorescence Lifetime of Parinaric Acid—To test the effect of environment on parinaric acid excited state lifetime, the probe was characterized in several systems. Below the critical micellar concentration (1 μM *cis*-parinaric acid), distributional analysis of phase and modulation data for *cis*-parinaric acid in ethanolic solution displayed three lifetime components near 1.0, 2.1, and 22.8 ns with fractional intensities of 0.43, 0.42, and 0.07, respectively (Table VII). Similar values were found for *trans*-parinaric acid. Above the critical micellar concentration (10 μM in ethanol), the distribution of the *cis*-parinaric lifetimes was changed. The long lifetime component was shifted to 55 ns, whereas the centers of lifetime distribution

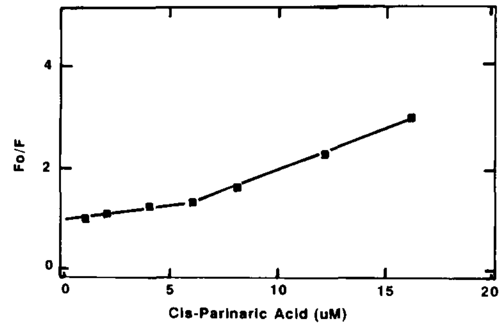

FIG. 8. **Quenching of I-FABP tryptophan fluorescence by *cis*-parinaric acid: Stern-Volmer plot.** The effect of increasing concentrations of *cis*-parinaric acid on I-FABP (4.3 μM) tryptophan fluorescence was determined as described under "Experimental Procedures." Data were plotted as a Stern-Volmer plot, where F_0 and F represent the fluorescence of I-FABP tryptophan in the absence and presence of *cis*-parinaric acid, respectively.

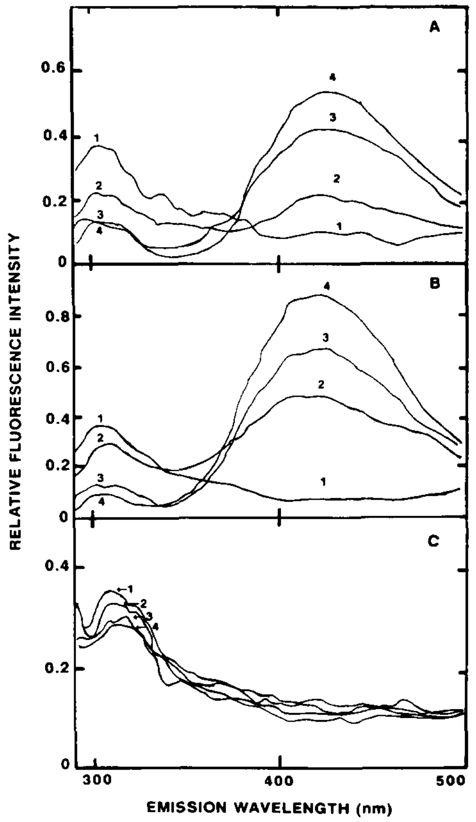

FIG. 9. **Effect of fatty acid binding on fluorescence emission spectra of L-FABP.** Fluorescence emission spectra of L-FABP (4.5 μM) in the presence of fatty acid were obtained as described under "Experimental Procedures." L-FABP was excitated at 285 nm. In *A*, *curves 1–4* had 0, 0.4, 1.6, and 3.2 μM *cis*-parinaric acid, respectively. In *B*, *curves 1–4* had 0, 0.2, 0.8, and 3.2 μM *trans*-parinaric acid, respectively. In *C*, *curves 1–4* had 0, 0.2, 0.8, and 3.8 μM oleic acid, respectively. All curves were corrected for background (fatty acid in buffer).

TABLE VII
Fluorescence lifetime analysis of cis- and trans-parinaric acids bound to I-FABP or L-FABP

Fluorescence lifetime distributional analysis was performed as described under "Experimental Procedures." Nonlinear least-squares analysis of the phase and modulation data yielded three lifetimes and fractional fluorescence similar to those obtained by distributional analysis. Distributional width is not listed below since it was maintained constant to resolve three components and three functions. *cis*-Parinaric acid and *trans*-parinaric acid concentrations were 0.5 μM unless otherwise stated. Palmitoyloleoylphosphatidylcholine (POPC)/cholesterol vesicles were present at a 65:35 mole ratio (2 μM in phosphate-buffered saline). I-FABP and L-FABP were 5 and 2.5 μM, respectively.

System	Centers of lifetime distribution			Fractional fluorescence		
	C_1	C_2	C_3	f_1	f_2	f_3
		ns				
cis-Parinaric acid						
1 μM in EtOH	22.78	2.07	1.08	0.07	0.416	0.43
10 μM in EtOH	55.05	2.18	0.72	0.09	0.40	0.51
POPC/cholesterol	9.61	2.38	0.24	0.85	0.13	0.02
I-FABP	7.60	2.16	0.27	0.23	0.30	0.46
L-FABP	5.15	2.03	0.63	0.38	0.44	0.18
trans-Parinaric acid						
I-FABP	7.19	2.15	0.25	0.30	0.38	0.31
L-FABP	5.68	2.15	0.42	0.25	0.61	0.15

of the short and intermediate lifetime components were unaltered. Fractional intensities of the various components were nearly the same above and below the critical micellar concentration. The results in Table VII further show that the center of distribution of the long lifetime component of *cis*-parinaric acid was sensitive to environmental changes. The center of lifetime distribution of the *cis*-parinaric acid long lifetime component decreased to 9.6 ns and fractional intensity increased to 0.85 when the *cis*-parinaric acid resided in palmitoyloleoylphosphatidylcholine/cholesterol (65 mol/35 mol) small unilamellar vesicle lipid bilayer (Table VII). The short lifetime component near 1.1 ns decreased to 0.2 ns (fractional intensity of 0.02), whereas the intermediate lifetime component near 2.1 ns was much less affected.

Fluorescence Lifetime of Bound Parinaric Acid—Multifrequency phase and modulation fluorometry and Lorentzian distributional analysis were used to examine the effect of I-FABP binding on excited state properties of the parinaric acid probes when parinaric acid was excited at 324 nm. The centers of lifetime distribution of *cis*-parinaric acid bound to I-FABP are 7.6, 2.1, and 0.27 ns, respectively; those of *trans*-parinaric acid bound to I-FABP were similar (Table V). Fractional fluorescence intensities of the three components were near 0.23, 0.30, and 0.46, respectively. Thus, in the I-FABP fatty-acid binding site, both *cis*- and *trans*-parinaric acids appear to reside in a hydrophobic environment with centers of lifetime distribution similar to those in membrane vesicles. However, the fractional contribution of the shorter lifetime components was greater when the fatty acids were bound to I-FABP than in membrane vesicles. These observations were also substantiated by the sensitized emission data in Table III.

The three lifetime components of *cis*-parinaric acid bound to L-FABP were similar to those in I-FABP except that the longer lifetime component additionally decreased 0.63 ns in L-FABP as compared to I-FABP (Table VII). Similar observations were apparent for *trans*-parinaric acid binding to L-FABP. As for I-FABP, *cis*- and *trans*-parinaric acids appear to reside in hydrophobic microenvironments in the L-FABP fatty acid-binding sites.

Static and Dynamic Properties of Bound Parinaric Acid—Steady-state anisotropy of bound *cis*- or *trans*-parinaric acid reflects the degree to which the FABP fatty acid-binding site restricts the mobility of fatty acid motion. The measured steady-state anisotropy is consistent with restricted motion of the fluorescent fatty acids in the binding site of both FABPs (Table VIII). This restriction seems somewhat larger (higher anisotropy) for *cis*-parinaric acid bound to either I-FABP or L-FABP. Since steady-state anisotropy is a mixed parameter composed of both static and dynamic components, differential polarized phase and modulation fluorometry was used to resolve the steady-state anisotropy into a static parameter, limiting anisotropy, and a dynamic parameter, rotational correlation time. As shown in Table VIII, the limiting anisotropies of *cis*- and *trans*-parinaric acids bound to I-FABP and L-FABP did not differ.

Rotational correlation time measured by the Perrin equation or by differential phase and modulation fluorometry was in the range of 3–6 ns, in a good agreement with previous determinations on L-FABP-bound anthroyl fatty acid analogs or with estimations by a spherical model with low molecular mass (14–15 kDa) with varying degrees of hydration. The Perrin equation was developed to describe the rotational behavior of fluorophores exhibiting isotropic motion in three dimensions and has frequently been applied to small globular proteins. In contrast, differential polarized phase and modulation fluorometry does not make the assumptions (isotropic motion and small globular protein) made by the Perrin equation. Nevertheless, both methods were in reasonably close agreement (Table VIII). These rotational correlation times were in the range of 4–5 ns, depending on which parinaric acid was bound to I-FABP or L-FABP (Table VIII).

DISCUSSION

The results presented herein focus on two fatty acid-binding proteins (I-FABP and L-FABP). Although these two fatty acid-binding proteins show high homology in cDNA sequence (50–52), their amino acid sequence homology is only 20% (52). The hydropathy index of these proteins differs considerably in the carboxyl-terminal region (Fig. 10). Only two amino acid sequences of these two proteins have a similar hydropathic index: residues 6–34 and 43–48. Thus, one might predict considerable differences in tertiary structure and ligand binding. Evidence consistent with such a prediction is as follows.

Binding Stoichiometry and Affinity—The number of fatty acid-binding sites and specificity were examined earlier with [^{3}H]oleic acid and *cis*- and *trans*-parinaric acids (30). Significantly, all three fatty acids (with two different binding assays) showed the presence of one binding site in I-FABP. It is possible that, even below the critical micellar concentration, the fatty acids may dimerize and that this could affect the binding stoichiometries and/or structural data presented herein. It should be emphasized that if the fluorescent fatty acids dimerized in solution, they would be self-quenched and, because of the absence of the putative dimer signal, would not contribute to the measurements made in this and earlier (30) studies. The importance of FABPs to cellular fatty acid metabolism is underscored by the toxic effects of unbound free fatty acids (1–6, 53). The binding stoichiometries observed for I-FABP above are in agreement with those generally agreed upon (18, 19, 21, 28). The content of I-FABP in intestine is 2% (1–6, 53). From the observed K_d values (near 1 μM) and these data, the total fatty acid binding capacity of the I-FABPs can be estimated to be 1.4 mM in intestine. Since the molar ratio of endogenously bound fatty acids varied

TABLE VIII

Dynamic and static properties of cis- and trans-parinaric acids bound to L-FABP and I-FABP

Protein and fatty acid concentrations used were as follows: FABPs, 5 μM; *cis*-parinaric acid, 0.5 μM; and *trans*-parinaric acid, 0.5 μM. Values represent the mean ± S.E. (n = 3).

	L-FABP		I-FABP	
	cis-Parinaric acid	*trans*-Parinaric acid	*cis*-Parinaric acid	*trans*-Parinaric acid
Anisotropy				
Steady-state	0.220 ± 0.005	0.203 ± 0.008	0.221 ± 0.012	0.208 ± 0.009
Limiting	0.120 ± 0.009	0.118 ± 0.015	0.132 ± 0.024	0.149 ± 0.016
Rotational correlation time				
Perrin equation (ns)[a]	5.4 ± 0.2	4.2 ± 0.2	5.3 ± 0.5	4.5 ± 0.3
Phase fluorometry (ns)[b]	4.0 ± 0.2	3.4 ± 0.2	5.1 ± 0.7	4.5 ± 0.4

[a] Rotational correlation time was calculated using the Perrin equation ($r_0/r = \mathrm{I} + (\tau/\phi)$), where r_0 was assumed to be 0.324 and τ was the fraction weighted average of the three parinaric acid lifetimes.

[b] The rotational correlation time was obtained by differential polarized phase fluorometry as described under "Experimental Procedures."

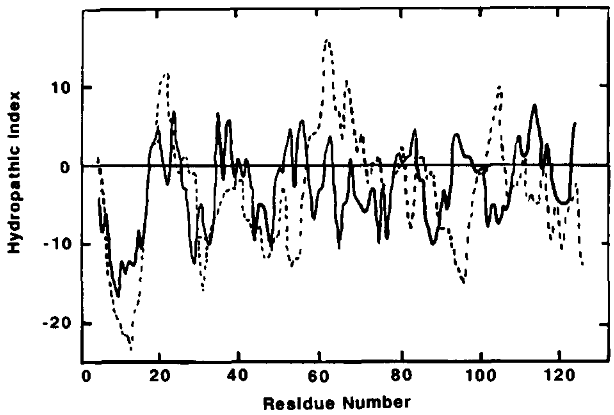

FIG. 10. **Hydropathy profiles of L-FABP and I-FABP.** Shown are Kyte-Doolittle hydropathy indices of L-FABP (——) and I-FABP (– – –) determined by the Kyte-Doolittle method as described earlier (26, 49).

between 0.4 and 1.3 mol/mol for these FABPs (reviewed in Ref. 53), the I-FABP-bound fatty acid concentration can be estimated to be 0.6–1.8 mM in intestine. This high binding capacity by FABPs would diminish the potential toxicity of nonesterified fatty acids inside the enterocyte. With regard to relative affinities for specific fatty acids, I-FABP exhibited higher affinities for unsaturated and polyunsaturated radiolabeled fatty acids than for saturated fatty acids (28, 30). This preference was confirmed with *trans*-parinaric acid (a straight chain or saturated fatty acid analog) and *cis*-parinaric acid (a kinked chain or unsaturated fatty acid analog) (30).

Both radiolabeled and fluorescent fatty acids showed the presence of two binding sites in L-FABP. Advantage was taken of the self-quenching properties of parallel oriented parinaric acids (54, 55) to examine the orientation of the two fatty acid-binding sites in L-FABP. If both fluorescent fatty acids bind in the same site or in sites oriented in parallel, their fluorescence would be self-quenched. This was not observed. The binding stoichiometry observed for L-FABP above is in agreement with that generally agreed upon (1–6, 53). The content of L-FABP in intestine and liver is 3 and 3–14%, respectively (1–6, 53). From the observed K_d values (near 1 μM) and these data, the total fatty acid binding capacity of L-FABP can be estimated to be 4.4 mM in intestine and 4–20 mM in liver. As calculated above, L-FABP-bound fatty acid concentration can be estimated to be 1.8–5.7 mM in intestine and 1.6–26 mM in liver. L-FABP exhibited higher affinities for unsaturated and polyunsaturated radiolabeled fatty acids than for saturated fatty acids (28, 30). This preference was confirmed with *trans*- and *cis*-parinaric acids (30).

Microenvironment of Fatty Acid-binding Site—The effect of binding to FABPs on the spectral and lifetime properties of *cis*- and *trans*-parinaric acids was examined. The absorption spectrum of *cis*- and *trans*-parinaric acids is red-shifted (~1.8 and 1.2 nm at the two major absorbance maxima) when the molar ratio of fatty acid to I-FABP was changed from 2:1 to 1:5. This spectral shift occurred when parinaric acid moved from buffer into the protein pocket, which is less water-accessible. The lifetime values of *cis*-parinaric acid are also consistent with this possibility. Two of the three lifetime components were insensitive for the changes in environment and remained constant ~1 ns and below 1 ns, respectively. In contrast, the longer *cis*-parinaric acid lifetime component appears to be more influenced by the physical-chemical state of the environment. In vesicles or micelles, this component is longer than 20 ns and is shortened in a hydrophilic environment. This lifetime component was not shortened greatly when *cis*-parinaric acid was bound to I-FABP.

Several observations indicate that the fatty acid-binding sites are more exposed to the aqueous environment. 1) Parinaric acid absorption spectral shifts were not detected with parinaric acid binding to L-FABP. 2) The lifetime values of *cis*-parinaric acid are also consistent with this possibility. The longer *cis*-parinaric acid lifetime component appeared to be shortened significantly when *cis*-parinaric acid was bound to L-FABP as compared to I-FABP. This is consistent with the L-FABP-binding site being relatively more solvent-exposed.

The motional properties of the *cis*- and *trans*-parinaric acids bound to I-FABP indicate that the fatty acids' motion in the binding site is restricted. However, the bound *cis*-parinaric acid was slightly more restricted than the bound *trans*-parinaric acid. Similar data were observed with L-FABP. Thus, it is likely that the L-FABP fatty acid-binding sites may also be "bent" as is the I-FABP-binding site (19) to accommodate the unsaturated fatty acid *cis*-double bonds. This would also restrict the mobility of the unsaturated fatty acids more than the saturated or straight chain fatty acids (*e.g. trans*-parinarate).

Proximity Relationships of Fatty Acids and FABP Aromatic Acids—The fluorescence spectral properties of I-FABP aromatic acids were examined in response to fatty acid binding. Several parameters indicated close proximity of the fatty acid to I-FABP tryptophan. This proximity was closer and tighter for *cis- versus trans*-parinaric acid. Acrylamide quenching and lifetime data indicate that only 1 of the 2 I-FABP tryptophans was in the fatty acid-binding site. Energy transfer from I-FABP tryptophan to parinaric acid indicates the calculated distance between them (R = 16.9–18.6 Å). The quenching of I-FABP tryptophan by parinaric acids indicates a distribution of tryptophan residues outside the 16.3-Å radius calculated for a 15.1-kDa (28) spherical protein (56). Since the fatty acids enter the binding site of I-FABP with the carboxyl-terminal end deeply buried in the interior (18–20), the fluorophore of the parinaric acid should be near the outer edge of the protein-binding pocket, with the I-FABP tryptophan residues located at the opposite end of the clam-shaped I-FABP molecule, a conclusion substantiated by x-ray crystal data (19).

The fluorescence spectral properties of L-FABP tyrosine were examined in response to fatty acid binding. Several parameters indicated close proximity of the fatty acid to the tyrosines. This proximity was closer and tighter for *cis- versus trans*-parinaric acid. Acrylamide quenching and lifetime data indicate that at least 1 tyrosine appears located in the L-FABP fatty acid-binding site. Although the quantum yield of tyrosine is approximately 6 times less compared to tryptophan, the quenching of L-FABP tyrosine by *cis*- or *trans*-parinaric acid is significant, such that the distance between them was 19.2 and 17.7 Å for bound *cis*- and *trans*-parinaric acids, respectively. In L-FABP, the fatty acid binds with the nonpolar tail buried within the hydrophobic binding pocket (21). Since the parinaric acid fluorophore is located nearer the methyl terminus of the fatty acid, the observed quenching of L-FABP tyrosine by the parinaric acids is consistent with an estimated non-uniform distribution of the tyrosine residues within the 16-Å radius expected for a 14.3-kDa protein (56). Thus, L-FABP is also likely to be spherical in shape.

In summary, the distance (R) between tyrosine and the parinaric acid-conjugated double-bound fluorophore seems to be very similar in L-FABP as compared to tryptophan and parinaric acid in I-FABP. Although x-ray data on holo L-FABP are not available, differences were observed between I-FABP and L-FABP in terms of the binding locations of their bound fatty acid carboxyl groups using ^{13}C NMR spectroscopy. At neutral pH, the carboxyl chemical shift was lower for fatty acid bound to I-FABP than for fatty acid bound to L-FABP. This observation suggested that the binding environment in I-FABP is less solvent-accessible than that in L-FABP.

FABP Conformational Changes upon Ligand Binding—The data presented herein indicate that I-FABP does not undergo significant conformational change upon fatty acid binding. The emission spectrum, second derivative absorbance spectra, and tryptophan lifetime data presented herein were not significantly changed upon nonfluorescent fatty acid binding. This observation is consistent with x-ray crystallographic evidence indicating little difference in the conformation of apo and holo I-FABPs containing bound palmitic acid (18, 19, 21). More important, the results presented herein with FABPs in aqueous solution substantiate those obtained with crystalline protein, indicating that crystallization did not grossly alter the conformation of the protein in solution.

In contrast, L-FABP appears to undergo significant conformational change upon fatty acid binding. Second derivative absorbance spectroscopy data reflected an increased polarity of the tyrosine environment upon oleic acid binding to L-FABP. Conformational changes in L-FABP upon fatty acid binding have also been observed as increased reactivity of cysteine 69 to 5,5′-dithiobis(nitrobenzoic acid) (57) and complex-induced circular dichroism spectra (2, 21). Preliminary x-ray data on apo, but not holo, L-FABP crystal structure were recently reported (22), but comparisons are not yet possible.

Conclusions—In summary, the data indicate that the fatty acid-binding sites of I-FABP and L-FABP differ considerably in structure, and the fatty acids are in a less polar binding site in I-FABP than in L-FABP. In addition, the occupancy of the fatty acid-binding site induces conformational changes in L-FABP, but not in I-FABP. Such conformational changes could be crucial for exposure of tyrosine, serine, or threonine residues to protein kinases. Phosphorylation of another fatty acid-binding protein, adipocyte FABP, is thought to be involved in signal transduction from the insulin receptor to the nucleus (14, 15). Thus, phosphorylation of tyrosine residues and fatty acid binding may be linked in some, but not all, FABPs, possibly differentiating fatty acid carrier and/or second messenger functions for these proteins.

Acknowledgments—We are very grateful to Dr. John B. Lowe for providing the bacterial strains expressing rat L-FABP and I-FABP. The expert assistance of Timothy Hubbell in purifying the proteins was much appreciated. We thank Dr. J. Ball for the use of the SLM Aminco SPF 500 fluorescence spectrophotometer and Drs. E. Gratton, W. Mantulin, M. VanDeven, and J. Mattheis (Laboratory for Fluorescence Dynamics) for providing invaluable assistance and instrumentation for measuring tryptophan lifetime. We also thank Dr. M. Eftink for his invaluable help by providing the program for acrylamide quenching analysis and especially for critical reading of the manuscript.

REFERENCES

1. Clarke, S. D., and Armstrong, M. K. (1989) *FASEB J.* **3,** 2480–2487
2. Spener, F., Börchers, T., and Mukherjia, M. (1989) *FEBS Lett.* **244,** 1–5
3. Schroeder, F., Butko, P., Nemecz, G., Jefferson, J. R., Powell, D., Rymaszewski, Z., Dempsey, M. E., Kukowska-Latallo, J., and Lowe, J. B. (1989) in *Bioengineered Molecules: Basic & Clinical Aspects* (Verna, R., Blumenthal, R., and Frati, L., eds) pp. 29–45, Raven Press, New York
4. Bass, N. M. (1988) *Int. Rev. Cytol.* **3,** 143–184
5. Sweetser, D. A., Heuckeroth, R. O., and Gordon, J. I. (1987) *Annu. Rev. Nutr.* **7,** 337–359
6. Glatz, J. F. C., and Veerkamp, J. H. (1985) *Int. J. Biochem.* **17,** 13–22
7. Weinberger, C., and Bradley, D. J. (1990) *Annu. Rev. Physiol.* **52,** 823–840
8. O'Malley, B. (1990) *Mol. Endocrinol.* **4,** 363–369
9. Bordewick, U., Heese, M., Börchers, T., Robenek, H., and Spener, F. (1989) *Biol. Chem. Hoppe-Seyler* **370,** 229–238
10. Bassuk, J. A., Tsichlis, P. N., and Sorof, S. (1987) *Proc. Natl. Acad. Sci. U. S. A.* **84,** 7547–7551
11. Custer, R. P., and Sorof, S. (1984) *Proc. Natl. Acad. Sci. U. S. A.* **81,** 6738–6742
12. Bohner, F. D., Kraft, R., Otto, A., Wernstedt, C., Hellman, U., Kurtz, A., Muller, T., Rohde, K., Etzold, G., Lehman, W., Langen, P., Heldin, C.-H., and Grosse, R. (1987) *J. Biol. Chem.* **262,** 15137–15143
13. Brandt, R., Pepperle, M., Otto, A., Kraft, R., Boehner, F.-D., and Grosse, R. (1988) *Biochemistry* **27,** 1420–1425
14. Yang, V. W., Christy, R. J., Cook, J. S., Kelly, T. K., and Lane, M. D. (1989) *Proc. Natl. Acad. Sci. U. S. A.* **86,** 3629–3633
15. Hresko, R. C., Bernier, M., Hoffman, R. D., Flores-Riveros, V. R., Liao, K., Larrid, D. M., and Lane, M. D. (1988) *Proc. Natl. Acad. Sci. U. S. A.* **85,** 8835–8839
16. Keuper, H. J. K., Klein, R. A., and Spener, F. (1985) *Chem. Phys. Lipids* **38,** 159–173
17. Gordon, J. I., and Lowe, J. B. (1985) *Chem. Phys. Lipids* **38,** 137–158
18. Sacchettini, J. C., Gordon, J. I., and Banaszak, L. J. (1989) *Proc. Natl. Acad. Sci. U. S. A.* **86,** 7736–7740
19. Sacchettini, J. C., Gordon, J. I., and Banaszak, L. J. (1989) *J. Mol. Biol.* **208,** 327–339
20. Sacchettini, J. C., Gordon, J. I., and Banaszak, L. J. (1988) *J. Biol. Chem.* **263,** 5815–5819
21. Cistola, D. P., Sacchettini, J. C., Banaszak, L. J., Walsh, M. T., and Gordon, J. I. (1989) *J. Biol. Chem.* **264,** 2700–2710

22. Winter, N. S., Gordon, J. I., and Banaszak, L. J. (1990) *J. Biol. Chem.* **265,** 10955–10958
23. Schroeder, F., Holland, J. F., and Vagelos, P. R. (1976) *J. Biol. Chem.* **251,** 6739–6746
24. Sklar, L. A., Hudson, B. S., and Simoni, R. D. (1975) *Proc. Natl. Acad. Sci. U. S. A.* **72,** 1649–1653
25. Sklar, L. A., Hudson, B. S., and Simoni, R. D. (1977) *Biochemistry* **16,** 5100–5108
26. Sklar, L. A., Doody, M. C., Gotto, A. M., and Pownall, H. J. (1980) *Biochemistry* **19,** 1294–1301
27. Lowe, J. B., Strauss, A. W., and Gordon, J. I. (1984) *J. Biol. Chem.* **259,** 12696–12704
28. Lowe, J. B., Sacchettini, J. C., Laposta, M., McQuillan, J. J., and Gordon, J. I. (1987) *J. Biol. Chem.* **262,** 5931–5937
29. Glatz, J. F. C., and Veerkamp, J. H. (1983) *Anal. Biochem.* **132,** 89–95
30. Nemecz, G., Hubbell, T., Jefferson, J. R., Lowe, J. B., and Schroeder, F. (1991) *Arch. Biochem. Biophys.* **286,** 300–309
31. Bradford, M. M. (1976) *Anal. Biochem.* **72,** 218–254
32. Cistola, D. P., Walsh, M. T., Corey, R. P., Hamilton, J. A., and Brecher, P. (1988) *Biochemistry* **27,** 711–717
33. Ragone, R., Colonna, G., Balestrieri, C., Servillo, L., and Irace, G. (1984) *Biochemistry* **23,** 1871–1875
34. Jefferson, J. R., Hunt, J. B., and Ginsburg, A. (1990) *Biochemistry* **29,** 6687–6698
35. Lakowicz, J. R. (1983) *Principles of Fluorescence Spectroscopy*, pp. 257–302, Plenum Press, New York
36. Eftink, M. R., and Ghrion, C. A. (1981) *Anal. Biochem.* **114,** 199–227
37. Forster, T. H. (1959) *Faraday Soc. Trans.* **27,** 7–17
38. Schroeder, F., Dempsey, M. E., and Fischer, R. T. (1985) *J. Biol. Chem.* **260,** 2904–2911
39. Fischer, R. T., Cowlen, M. S., Dempsey, M. E., and Schroeder, F. (1985) *Biochemistry* **24,** 3322–3331
40. Steinberg, I. Z. (1971) *Annu. Rev. Biochem.* **40,** 83–114
41. Stryer, L. (1978) *Annu. Rev. Biochem.* **47,** 819–846
42. Haas, E., Katzin, E. K., and Steinberg, I. Z. (1978) *Biochemistry* **17,** 5064–5070
43. Dale, R. E., Eisinger, J., and Blumberg, W. E. (1979) *Biophys. J.* **26,** 161–194
44. Ludescher, R. D., Volwerk, J. J., Hass, G. H., and Hudson, B. S. (1985) *Biochemistry* **24,** 7240–7249
45. Nemecz, G., and Schroeder, F. (1988) *Biochemistry* **27,** 7740–7749
46. McIntyre, J. C., Schroeder, F., and Behnke, W. E. (1990) *Biochemistry* **29,** 2092–2101
47. Burstein, E. A., Vedenkina, N. S., and Ivkova, M. N. (1973) *Photochem. Photobiol.* **18,** 263–279
48. Ross, J. A., Schmidt, C. J., and Brand, L. (1981) *Biochemistry* **20,** 4369–4377
49. Bismuto, E., Irace, G., and Gratton, E. (1989) *Biochemistry* **28,** 1508–1512
50. Gordon, J. I., Alpers, D. H., Ockner, R. K., and Strauss, A. W. (1983) *J. Biol. Chem.* **258,** 3356–3363
51. Alpers, D. H., Strauss, A. W., Ockner, R. K., Bass, N. M., and Gordon, J. I. (1984) *Proc. Natl. Acad. Sci. U. S. A.* **81,** 313–317
52. Lowe, J. B., Boguski, M. S., Sweetser, D. A., Elshourbagy, N. A., Taylor, J. M., and Gordon, J. I. (1985) *J. Biol. Chem.* **260,** 3413–3417
53. Paulussen, R. J. A., and Veerkamp, J. H. (1990) in *Subcellular Chemistry: Intracellular Transfer of Lipid Molecules* (Hilderson, H. J., ed) Vol. 16, pp. 175–226, Plenum Press, New York
54. Van Loon, D., Berkhout, Th. A., Demel, R. A., and Writz, K. W. A. (1985) *Chem. Phys. Lipids* **38,** 29–39
55. Berkhout, T. H. A., Visser, A. J. W. G., and Wirtz, K. W. A. (1984) *Biochemistry* **23,** 1505–1513
56. Cantor, C. R., and Schimmel, P. R. (1980) *Biophysical Chemistry*, Part II, pp. 459–463, W. H. Freeman & Co., New York
57. Wilton, D. C. (1989) *Biochem. J.* **261,** 273–276